Assimilation of satellite data over Saharian desert for intercalibration of optical satellite sensors

Miesch C.[*a], Cabot F.[**b], Briottet X.[a], Henry P.[b]
[a]Office National d'Etudes et de Recherches Aérospatiales (Toulouse, France);
[b]Centre Nationale d'Etudes Spatiales (Toulouse, France)

ABSTRACT

About twenty Saharian desert regions have been selected a few years ago in order to carry out in-flight calibration of the different instruments operating in the visible and near-infrared spectral domain. Since then, CNES has collected an important number of measurements acquired by these instruments of interest (SPOT, AVHRR, SeaWiFS, Polder, Vegetation, MODIS, MISR) over the selected desert areas (SADE database).
The present work fits into a global assimilation approach which aims to improve both the characterization of the calibration sites and the cross-calibration of optical satellite sensors. This work is particularly devoted to the spectral characterization of the selected site using the SADE database. The method is based on the use of a spectral model of ground surface reflectance at global scale. It is assumed that this model can be derived from laboratory reflectance measurement (i.e. "small scale" measurement). Then, instead of reversing the top of atmosphere measurement into ground reflectance, the ground reflectance model is transported at the top of atmosphere for comparison to available measurement, and the parameters adjustment is done at this level. A top of atmosphere simulated reflectance dataset (corresponding to various usual multispectral sensors) is used in a first step to assess for the relevancy of the proposed method.

Keywords: calibration, desert sites, reflectance, satellite measurements database SADE.

1. INTRODUCTION

Various Saharian regions have been selected[1] a few years ago in order to carry out an in-flight calibration of the different instruments operating in the visible and near-infrared spectral domain. The CNES (Centre National d'Etudes Spatiales) has collected an important number of measurements taken by these instruments of interest (e.g., SPOT, AVHRR, SeaWiFS, Polder, Vegetation, MODIS, MISR) over these selected areas with the purpose to develop an assimilation method able to improve both reference sites (i.e. the previous selected desert region) characterization and calibration coefficients of optical sensors. All these data are stored in the SADE ("Structure d'Accueil pour les Données d'Etalonnage") database[2], the goal of which is to feed the assimilation method. This method is based on the iteration of an algorithm that can be summarized by the following figure:

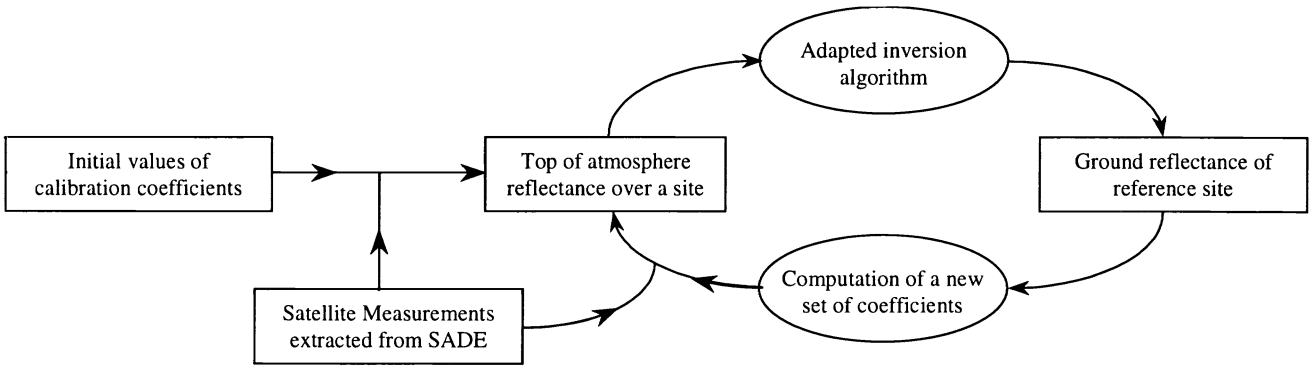

Figure 1: Iteration algorithm of the assimilation method.

* christophe.miesch@onecert.fr; phone +33 5 62 25 26 51, fax +33 5 62 25 25 88; ONERA, 2, avenue Edouard Belin, 31055 TOULOUSE Cedex, France
** francois.cabot@cst.cnes.ft; phone +33 5 61 27 33 04, fax +33 5 61 27 31 67; CNES, 18, avenue Edouard Belin, 31400 TOULOUSE

Sensors, Systems, and Next-Generation Satellites V, Hiroyuki Fujisada,
Joan B. Lurie, Konradin Weber, Editors, Proceedings of SPIE Vol. 4540 (2001)

In a first step, a given reference site is chosen, and a set of satellite measurements over this site is extracted from the SADE database. Using initial values of calibration coefficients, the corresponding top of atmosphere reflectances can be computed. Then, an adequate inversion algorithm performs atmospheric corrections and inversion, in order to retrieve ground reflectance properties. Knowing these properties, direct atmospheric radiative transfer codes (like 6S for instance) allow to retrieve top of atmosphere reflectances, and a new set of calibration coefficients can be then computed. This process is iterated until an acceptable convergence is reached.
The present work focus on the so-called "Adapted inversion algorithm" step. As the problem is complex, it is simplified in a first step to the spectral behavior retrieval of the ground surfaces, i.e., the set of satellite measurements is chosen so that the directional angular configurations of them are almost identical (so that no directional effect is introduced). As there is an important variety of bands available, it is necessary to introduce a spectral model of the ground surface, with adapted parameters that need to be adjusted. The first part of this paper is devoted to the analysis of the spectral behavior of the desert site reflectance at large scale, using the assumption that this behavior is comparable to the one of the sands that constitute them. Then, an adapted adjustment method has to be performed. An original one is presented here, that considers the comparison of the modeled reflectances and the measured ones at satellite level, instead of ground level (which is usually what is done). The adjustment done at satellite level needs more computation time but allows to perform the atmospheric transfer wavelength by wavelength, and is thus much more correct than considering broad-band transfers. This adjustment is presented in the second part of this paper, and a preliminar result obtained with a simulated top of atmosphere reflectance dataset is presented to test the relevancy of method.

2. SPECTRAL MODEL

2.1. Reflectance measurements

The reflectance of a given surface depends on both the wavelength and geometrical properties of the incident beam and the viewing directions. At present, most of the bidirectional reflectance models work at a given wavelength, and do not consider it as a parameter (such as viewing zenith, for instance). In this paper, we will focus only on the spectral behavior of reflectances; however, it would be interesting if the global spectral behavior of the reflectance could be represented by a unique model (most probably with different adjustments) independently of the geometrical observation conditions. To check if this assumption is reasonable, we use a goniometer[3] to measure the spectral evolution of the reflectance for various geometric configuration. The spectrometer that equips the goniometer works from 450 nm up to 920 nm. and allows measurements up to 60° of zenith angles. Different spectral signatures corresponding to various geometrical configurations are plotted for sand of Algeria 4 on Figure 2; the three values associated for each plot give respectively the incident zenith angle, the viewing zenith angle and the relative azimuth.

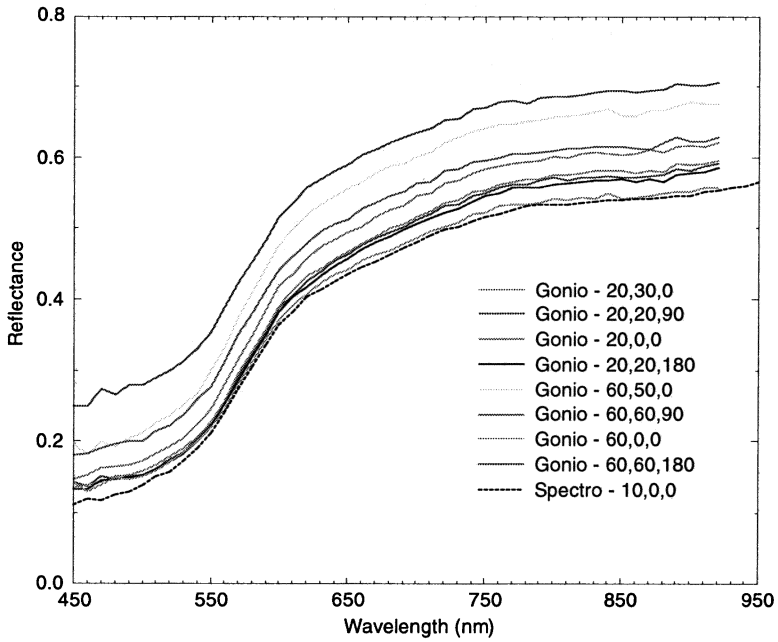

Figure 2: Spectral reflectances of sand from Algeria 4 site for various angular conditions.

All but one of these plots result from goniometer measurements; the last one was taken by a spectro-radiometer that have a larger working domain (0.4-2 µm) but that allows only one angular configurations (nadir-acquisition, incidence with a zenith angle of 10°). It appears clearly on Figure 2 that the spectral shape is very similar, whatever condition is taken: there is a clear increase of the reflectance value from 450 nm, with an inflexion point around 570°nm, and the increasing becomes slighter over 750°nm.
This first result is interesting, as it shows that the directional effects may be uncoupled from the spectral ones. Going further with this analysis, we introduce a significant roughness on the surface, as shown on Figure 3. The sand comes here from a Mediterranean beach, as we did not have enough from any of the desert. It appears much less reflecting, but have similar spectral shape.

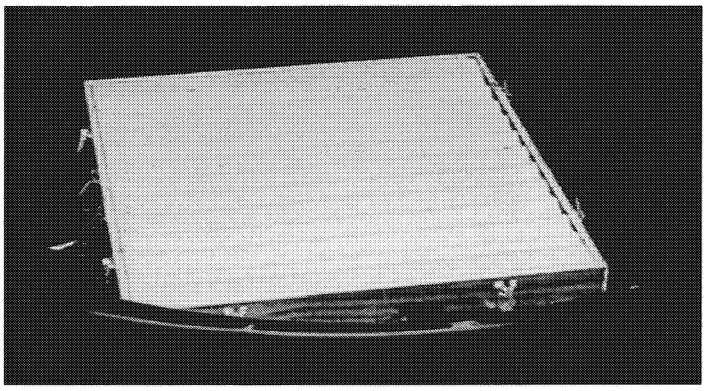

Figure 3: Sample of sand with a linear dunes-like shape.

The directional effects introduced by the dune are plotted on Figure 4. They appear to be much more important than without roughness on the surface; the backward reflection is still important, but the roughness introduces shadowing and specularity effects (on the slopes of dunes) that produce the reflectance on the right side of the principal plane to be weak and the reflectance on the left side to be greater. However, the spectral shape is not altered by the roughness, only reflectance levels are modified.

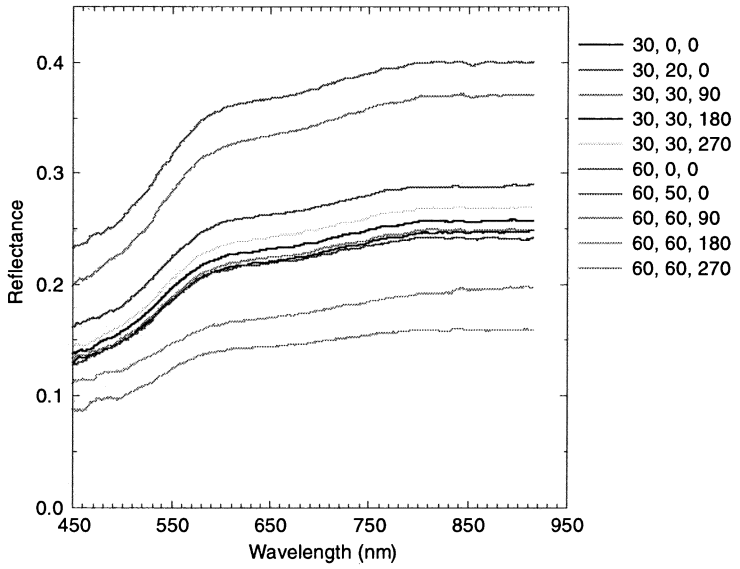

Figure 4: Spectral reflectances of linear dunes of sand for various angular conditions.

In the last measurement set, a variety of desert sands are considered, and characterized by the spectro-radiometer (that works from 400 to 2000 nm). Thus, the analysis focus on the spectral behavior of each sand. The measurement are plotted on Figure 5.
Again, the spectral shape are very similar, even if there are magnitude and offset differences between plots. The global behavior from 400 to 1800 nm can be summarized as follow: there is an important increase of the reflectance values from

450 to 750 nm, with an inflexion point around 570 nm; over 800 nm the increase is weaker; a local absorption peak is observed around 1400 nm, which comes from the hydroxide ion trapped in the silicates[4].

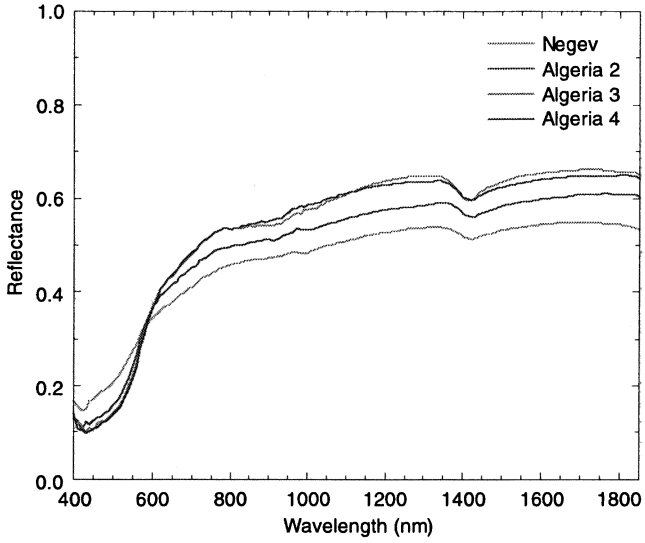

Figure 5: Spectral reflectances of some desert sands.

2.2. Model description and performances

In the case we neglect the absorption peak around 1400°nm, the global spectral behaviors of desert sands is simple, and the difference between various sands would be reduced to different levels of reflectance at 400 nm and around 1000 nm, and different positions and slopes of the inflexion point. A simple model adapted to this behavior could be defined as:

$$\rho^{\mathrm{mod}}(\lambda) = A \cdot \arctan(\alpha \cdot \lambda + \beta) + B \qquad (1)$$

This model reproduce the different part of the reflectance shape, except the peculiarity around 1400 nm. This peculiarity is however not important for our objectives as it is located outside of the bands of the optical sensors of interest.

The adjustment of the spectral model on spectral measurements may be done by minimizing the usual cost function corresponding to the root mean square relative error (RMSE) between the measured and modeled datasets:

$$f(A,B,\alpha,\beta) = \sqrt{\frac{1}{N}\sum_{i=1}^{N}\left[\frac{\rho^{\mathrm{mod}}(\lambda_i,A,B,\alpha,\beta) - \rho^{mes}(\lambda_i)}{\rho^{mes}(\lambda_i)}\right]^2} . \qquad (2)$$

The minimization of this function is done by usual methods, like Simplex for instance. However, in a real case, we will not have access to spectral data, but multispectral ones. So the available data will correspond to measurements taken in the response bands of usual instruments. Thus, the cost function that have to be used can be written:

$$f(A,B,\alpha,\beta) = \sqrt{\frac{1}{N}\sum_{i=1}^{N}\left[\frac{\int_0^{\infty} S_i(\lambda)\cdot\rho^{\mathrm{mod}}(\lambda,A,B,\alpha,\beta)\cdot d\lambda - \rho_i^{mes}}{\rho_i^{mes}}\right]^2} . \qquad (3)$$

where S_i is the spectral response of the instrument associated to the i^{th} measurement.

In a first, the model is adjusted on the spectral data (i.e. the used cost function is given in equation 2) obtained from the Algeria 4 sand (on the spectral domain 400-1800 nm, see Figure 6). The root mean square relative error is about 5% and the maximum error reaches 10% (around 590 nm). The absolute maximum error is 0.037.

However, it is most usual to have reflectance data acquired over broad bands. Thus, to check the performance of the adjustment (using this time equation 3), a reflectance dataset has been simulated thanks to the spectral reflectance of the sand from Algeria 4 site over various usual bands (SPOT/XS and MIR, VEGETATION, POLDER, AVHRR/RED and NIR, SeaWiFS/all except 412nm). A measurement was "rebuilt" for each band, by integrating the spectral reflectance. The results are plotted on Figure 7.

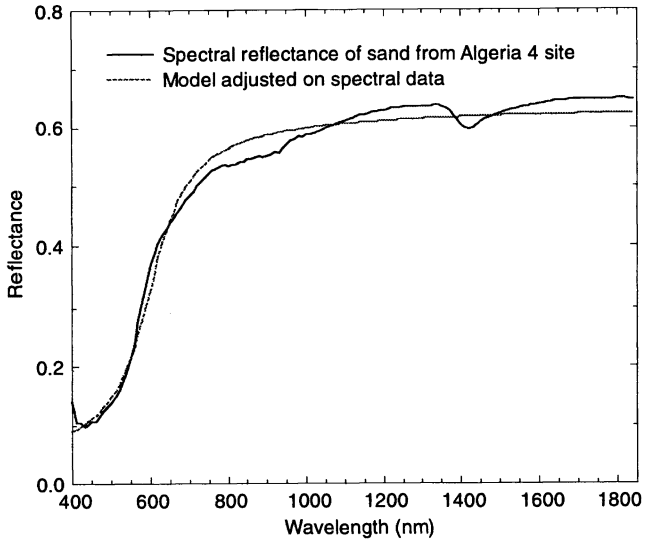

Figure 6: Model adjusted on the spectral reflectance of the sand from Algeria 4 site.

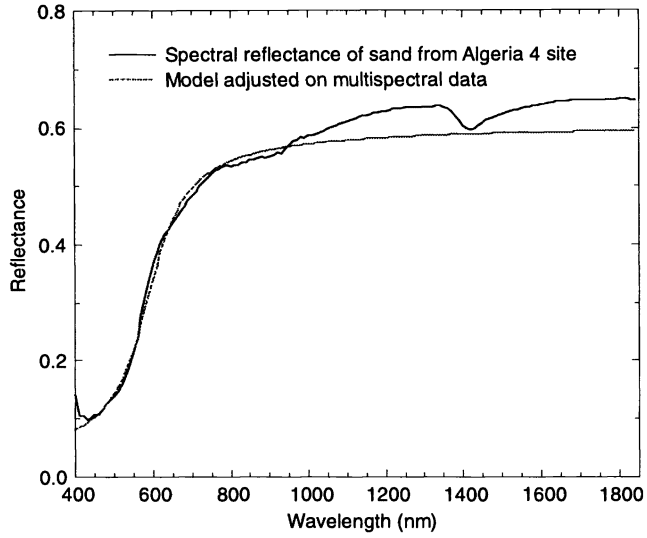

Figure 7: Model adjusted on a multispectral dataset issued from spectral reflectance of the sand from Algeria 4 site.

The root mean square relative error over the various band is less than 1.5%, with a maximum relative error of 8% (for the MIR band of VEGETATION and SPOT). When comparing spectrally the datasets, the root mean square relative error is slightly greater than for the previously adjusted model (around 5.5%), while the maximum relative error is still around 10%. However, the error is greater in the middle infrared, as there are less bands in this domain than in the visible one.
The errors computed in this example appears to be reasonable. Of course, more flexible models (polynomial or spline, for instance) would give better results; however, an important advantage of the simple "arctan" model resides in the fact that there are only four parameters, and each one of them plays a specific role (in the amplitude of variation, the global offset, the position and the slope of the inflexion point). This induces the model to be robust in term of the shape reproduced, even if some data are noisy.

3. ADJUSTMENT METHOD ON SATELLITE DATA

3.1. Description of the method

Satellite sensors are sensitive to radiance, that can be expressed in term of top of atmosphere reflectance. This signal can be expressed the following way:

$$\rho^{TOA}(\lambda)=\left\{\rho_{atm}(\lambda,\theta_s,\theta_v)+\frac{\rho^{ground}(\lambda)}{1-\rho^{ground}(\lambda)\cdot s_{atm}(\lambda)}\left(e^{-\tau/\mu_s}+t_d^{\downarrow}(\lambda,\theta_s)\right)\cdot\left(e^{-\tau/\mu_v}+t_d^{\uparrow}(\lambda,\theta_v)\right)\right\} \times T_{gatm}^{\downarrow\uparrow}(\lambda,\theta_s,\theta_v) \quad (4)$$

where $\rho_{atm}(\lambda,\theta_s,\theta_v,\Delta\phi)$ is the atmospheric intrinsic reflectance for an solar zenith angle of θ_s, a viewing zenith angle of θ_v and a relative azimuth angle of $\Delta\phi$; $\rho^{ground}(\lambda)$ is the ground reflectance (assumed lambertian), $s_{atm}(\lambda)$ is the spherical albedo of the atmosphere, τ is the total optical thickness of the atmosphere (without accounting gaseous absorption), μ_s et μ_v respectively the cosines of θ_s and θ_v, $t_d^{\downarrow}(\lambda,\theta_s)$ and $t_d^{\uparrow}(\lambda,\theta_v)$ respectively the downward and upward diffuse transmissions, and finally, $T_{gatm}^{\downarrow\uparrow}(\lambda,\theta_s,\theta_v)$ is the product of the gaseous transmissions of the downward and upward paths. For a given spectral band i characterized by the spectral response S_i, the top of atmosphere reflectance is then:

$$\rho_i^{TOA}=\int_0^{\infty}S_i(\lambda)\cdot\left(atm_1^i(\lambda)+\frac{\rho^{ground}(\lambda)}{1-\rho^{ground}(\lambda)\cdot atm_2^i(\lambda)}atm_3^i(\lambda)\right)\cdot d\lambda, \quad (5)$$

with:

$$\begin{cases} atm_1(\lambda)=\rho_{atm}(\lambda,\theta_s,\theta_v)\cdot T_{gatm}^{\downarrow\uparrow}(\lambda,\theta_s,\theta_v) \\ atm_2(\lambda)=s_{atm}(\lambda) \\ atm_3(\lambda)=\left(e^{-\tau/\mu_s}+t_d^{\downarrow}(\lambda,\theta_s)\right)\cdot\left(e^{-\tau/\mu_v}+t_d^{\uparrow}(\lambda,\theta_v)\right)\cdot T_{gatm}^{\downarrow\uparrow}(\lambda,\theta_s,\theta_v) \end{cases} \quad (6)$$

Introducing atmospheric models for each satellite measurements available in an extracted dataset over a given desert site (NCEP, TOMS and meteorological data are also available in the SADE database) and computing atm_1, atm_2 and atm_3 for each data over the corresponding spectral sensor response, the adjustment of the model can then be done by minimizing the function:

$$f(A,B,\alpha,\beta)=\sqrt{\frac{1}{N}\sum_{i=1}^{N}\left[\frac{\int_0^{\infty}S_i(\lambda)\cdot\left(atm_1^i(\lambda)+\frac{\rho^{\mathrm{mod}}(\lambda)}{1-\rho^{\mathrm{mod}}(\lambda)\cdot atm_2^i(\lambda)}atm_3^i(\lambda)\right)\cdot d\lambda-\rho_i^{mes}}{\rho_i^{mes}}\right]^2} \quad (7)$$

This function is obviously complex, but requires reasonable computation times even if it is evaluated a important number of times (as it is the case with minimization algorithm like Simplex).

3.2. Preliminary results

In order to check the method, a simulated dataset is generated at the top of atmosphere, thanks to the 6S radiative transfer code, for a ground reflectance supposed to be the one of the sand of Algeria 4 site, for a given angular configuration and a given atmospheric model. The dataset is generated for the same bands as the ones considered in section 2.2. A dataset of about forty reflectance values are then obtained, and are used with the adjustment method previously described. The result is plotted on Figure 8.

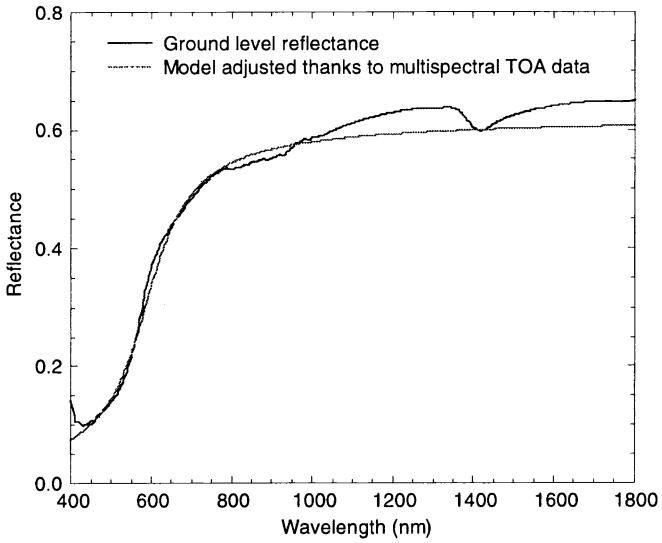

Figure 8: Ground level model adjusted with the simulated top of atmosphere dataset.

The model retrieved has very similar properties than the one retrieved after the multispectral adjustment performed in section 2.2. The root means square relative error is around 2% with a maximum absolute error encountered in the middle infrared. Even if this result is obtained for a "perfect" top of atmosphere dataset and with completely known atmospheric conditions, it show that the non linearity introduced by the atmospheric effects accounted for in the function to minimize has no significant effect on the adjustment.

4. FURTHER WORK

This work allows us to establish that a simple model (based on the "arctan" function) with few parameters appears to be in a first step well adapted to reproduce the spectral behavior of desert sand reflectances. Moreover, goniometer measurements taken for various angular configurations show that this spectral model can easily be used independently of the given geometrical configuration (the adjustment however will be specific for one angular configuration). With the assumption that this model is also relevant for desert observed at larger scale, this model is then introduced in an inversion method, in order to retrieve the spectral variations of the reflectance of desert reference sites. This method consists of adjusting the parameters of the spectral model by transferring the modeled reflectance to the top of atmosphere and comparing it to the measured reflectance dataset available. The method is tested on a top of atmosphere simulated dataset. While this test does not completely validate the method (the dataset is perfectly consistent and the atmospheric conditions are completely known), it shows that the atmospheric correction introduced in the function to minimize does not perturb significantly the minimization and that good results are retrieved.

In order to validate more completely the method, its robustness has to be further tested. So as to do this, a sensibility study will be performed on various parameters. The atmospheric conditions have to be considered as not well known, noise and uncertainty will be introduced in reflectance measurement, and finally, the influence of the spectral band availability has to be evaluated.

REFERENCES

1. Cosnefroy H., Leroy M. and Briottet X., "Selection and Characterization of Saharian and Arabian desert sites for the calibration of optical satellite sensors", Remote Sensing of Environment, Vol. 58, pp. 101-114, 1996.
2. Cabot, F., O. Hagolle, C. Ruffel, and P. Henry, "Use of remote sensing data repository for in-flight", Proceeding of SPIE, 1999, Denver, CO, USA, 1999.
3. Serrot G, Bodilis M., Briottet X. et Cosnefroy H, "Presentation of a new BRDF measurement device", Europto Series, "Atmospheric Propagation, Adaptive Systems, and Lidar Techniques for Remote Sensing II", 3494:23-33, Barcelona, 1998.
4. Guyot G., "Signatures spectrales des surfaces naturelles", Paradigme, 1989.